Respiratory Physiology & Neurobiology 266 (2019) 95–102

Contents lists available at ScienceDirect

Respiratory Physiology & Neurobiology

journal homepage: www.elsevier.com/locate/resphysiol

Excitation-inhibition balance regulates the patterning of spinal and cranial inspiratory motor outputs in rats *in situ*

Rishi R. Dhingra[a,*], Werner I. Furuya[a], Roberto F. Galán[b], Mathias Dutschmann[a,*]

[a] Division of Systems Neurophysiology, The Florey Institute of Neuroscience & Mental Health, Melbourne, Australia
[b] Department of Electrical Engineering and Computer Science, Case Western Reserve University, Cleveland, USA

ARTICLE INFO

Keywords:
Respiratory pattern formation
Distributed neural network
Excitation-inhibition balance
Respiratory microcircuit

ABSTRACT

Spinal phrenic nerve activity (PNA) drives the diaphragm but cranial hypoglossal nerve activity (HNA) also expresses synchronous activity during inspiration. Here, we investigated the effects of local disinhibition (bilateral microinjections of bicuculline) of the nucleus tractus solitarius (NTS), the pre-Bötzinger complex and Bötzinger complex core circuit (pre-BötC/BötC) and the Kölliker-Fuse nuclei (KFn) on the synchronization of PNA and HNA in arterially-perfused brainstem preparations of rats. To quantitatively analyze the bicuculline effects on a putatively distributed inspiratory central pattern generator (i-CPG), we quantified the phase synchronization properties between PNA and HNA. The analysis revealed that bicuculline-evoked local disinhibition significantly reduced the strength of phase synchronization between PNA and HNA at any target site. However, the emergence of desynchronized HNA following disinhibition was more prevalent after NTS or pre-BötC/BötC microinjections compared to the KFn. We conclude that the primary i-CPG is located in a distributed medullary circuit whereas pontine contributions are restricted to synaptic gating of synchronous HNA and PNA.

1. Introduction

Respiratory motor activities are expressed in a variety of functionally diverse muscles and muscle groups in order to modulate the depth and duration of inspiratory and particularly expiratory airflow (Bartlett, 1989; Dutschmann and Dick, 2012; Dutschmann and Paton, 2002; Sant'Ambrogio et al., 1995; Smith et al., 2013; Widdicombe, 1982). Briefly, respiration is governed by two motor systems: (i) the respiratory motor pools in the spinal cord govern respiratory pump muscles in the abdomen and thorax that generate pressure gradients to move air into or out of the lungs, and (ii) brainstem motoneurons supply muscles in the upper airways via specific branches of cranial nerves V, VII, IX X and XII that adjust and modulate airway resistance to determine the duration and/or force of pulmonary airflow. The complexity of respiratory motor activity is reflected in its motor pattern of inspiration, post-inspiration (controlled expiration, see (Dutschmann et al., 2014) and expiration (passive- or active-expiration, see Iscoe, 1998; Molkov et al., 2010; Pisanski and Pagliardini, 2018).

The pre-motor networks that generate the three-phase respiratory rhythm are thought to be localized within the ventrolateral medulla (Del Negro et al., 2018; Ramirez and Baertsch, 2018; Richter and Smith, 2014; Smith et al., 2009). However, recent evidence exists that the generation of the three-phase respiratory motor pattern depends on the rhythm-generating pool's embedding within a larger ponto-medullary network (Dhingra et al., 2019). This most recent study showed that local disinhibition of the nucleus tractus solitarius (NTS), the pre-Bötzinger/Bötzinger complexes or the Kölliker-Fuse nuclei, but not the mibrain periaqueductal gray, was sufficient to perturb global respiratory network dynamics thereby evoking a disruption of the alternation between inspiration and post-inspiration as observed in the primary motor pattern (Dhingra et al., 2019). We concluded (1) that the inspiratory off-switch mechanism is distributed across the ponto-medullary brainstem and is an emergent property of the rCPG network; and (2) that excitation-inhibition balance within and across nodes of the distributed rCPG network is a mechanism that underlies the generation of the eupneic respiratory motor pattern.

In the present study, we use similar experimental and analytical approaches to investigate whether the functional structure of the network regulating spinal and cranial inspiratory motor outputs in the phrenic and hypoglossal nerves, respectively, is equally as distributed as the network underlying inspiratory and post-inspiratory respiratory pattern formation. We show that while spinal and cranial inspiratory motor outputs are perturbed by local modulation of circuit excitability in the nucleus tractus solitarius (NTS), pre-Bötzinger complex/Bötzinger complexes (pre-BötC/BötC) or KFn, local disinhibition of medullary targets evokes a stronger disruption of the eupneic pattern of

* Corresponding authors.
E-mail addresses: rishi.dhingra@florey.edu.au (R.R. Dhingra), mathias.dutschmann@florey.edu.au (M. Dutschmann).

https://doi.org/10.1016/j.resp.2019.05.001
Received 13 February 2019; Received in revised form 11 April 2019; Accepted 2 May 2019
Available online 02 May 2019
1569-9048/

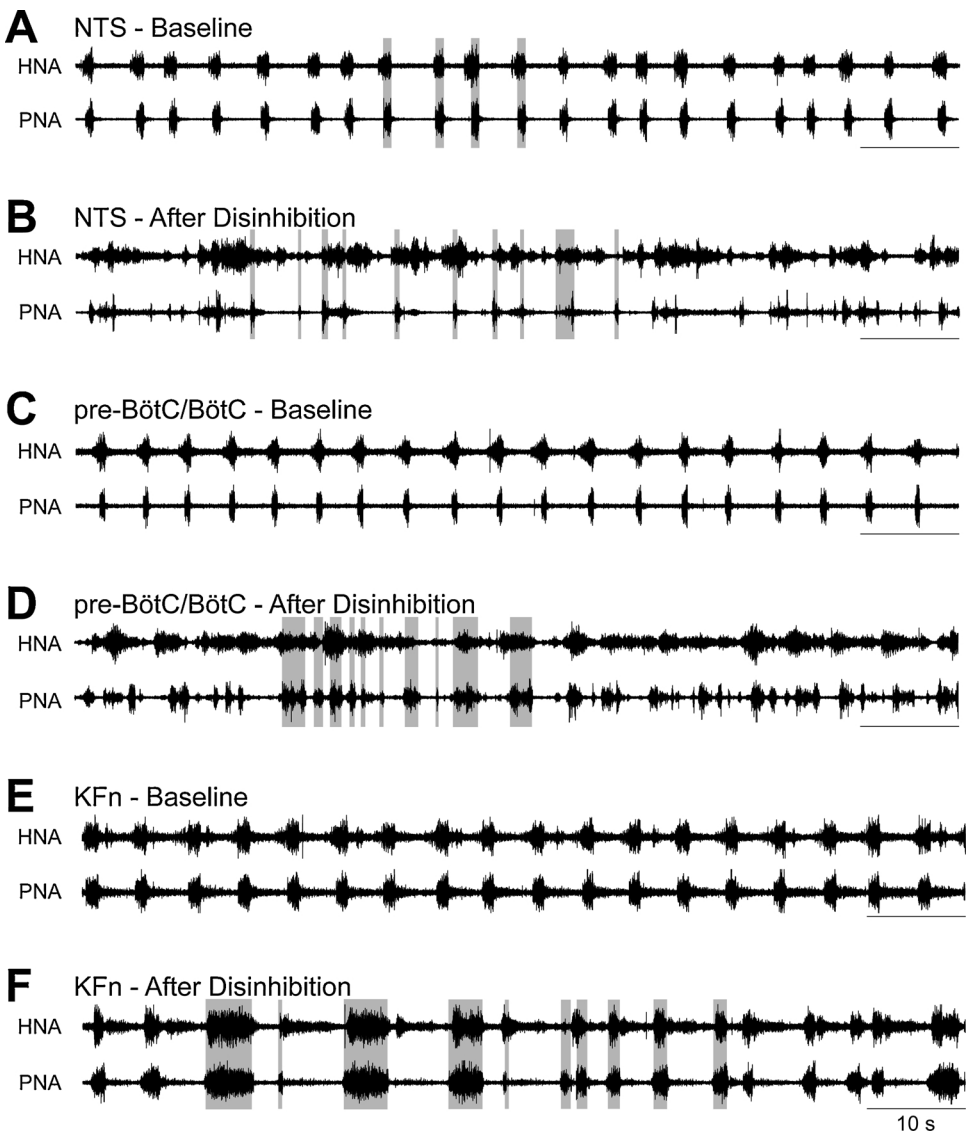

Fig. 1. Local disinhibition of brainstem respiratory nuclei perturbs the coupling of spinal and cranial inspiratory motor patterns. In the present study, we tested whether excitation-inhibition balance within the NTS, pre-BötC/BötC or KFn influences the generation of spinal phrenic (PNA, bottom traces) and cranial hypoglossal (HNA, top traces) inspiratory motor patterns by locally microinjecting the GABA(A)R antagonist bicuculline into one of the brainstem target sites. Representative traces are shown at baseline (A, C & E) and after local disinhibition of the NTS (B), pre-BötC/BötC (D) or KFn (F). At baseline (A, C & E), we observed the typical eupneic pattern of phrenic (PNA) and hypoglossal (HNA) nerve activities such that a cranial HNA inspiratory burst begins shortly before a spinal PNA inspiratory burst (*e.g.*, during pre-inspiration) and that both nerves continue to discharge simultaneously throughout the inspiratory phase of the breathing cycle. Shaded bars (in A, B, D & F) indicate periods where PNA is active, thereby highlighting the pre-inspiratory discharge in HNA observed at baseline (A). After local disinhibition of the NTS (B), spinal PNA inspiratory bursts became shorter in duration and more variable. Importantly, after local disinhibition of the NTS, HNA was enhanced in frequency and additional HNA bursts often occurred during periods when PNA was silent (compare HNA during and between shaded gray bars). After local disinhibition of the pre-BötC/BötC (D), PNA bursts and inter-burst intervals became even more variable. Like local disinhibition of the NTS, local disinhibition of the pre-BötC/BötC had a strong effect on HNA discharge such that HNA burst frequency was enhanced and additional HNA bursts often occurred out of phase with PNA. Finally, local disinhibition of the KFn (F) had a strong effect on inspiratory off-switch mechanisms such that PNA burst duration became highly variable. However, unlike local disinhibition of the NTS or pre-BötC/BötC, after local disinhibition of the KFn, cranial inspiratory HNA tended to discharge simultaneously with spinal inspiratory PNA.

hypoglossal nerve activity and of the phase synchronization between phrenic and hypoglossal nerve activity.

2. Materials and methods

Experimental protocols were approved by and conducted with strict adherence to the guidelines established by the Animal Ethics Committee of The Florey Institute of Neuroscience & Mental Health, Melbourne, Australia. Phrenic nerve recordings presented in this study comprised a subset of those published in a previous study (Dhingra et al., 2019).

2.1. Perfused brainstem preparation

Experiments were performed in juvenile Sprague-Dawley rats of either sex (N = 17 rats, 17–30 days post-natal) using the arterially perfused *in situ* brainstem-spinal cord preparation as described previously (Dhingra et al., 2017; Dutschmann et al., 2000; Paton, 1996). Briefly, rats were anesthetized by inhalation of isoflurane (2%) until they reached a surgical plane of anesthesia. The rats were then transected below the diaphragm and transferred to an ice-cold bath of artificial cerebrospinal fluid (aCSF, in mM: 125 NaCl, 3 KCl, 1.25 KH_2PO_4, 2.5 $CaCl_2$, 1.25 $MgSO_4$, 25 $NaHCO_3$, 10 D-glucose) for precollicular decerebration. After decerebration, the lungs and heart were removed. Next, the descending aorta, phrenic and hypoglossal nerves were dissected for subsequent cannulation or recording. The preparation was then transferred into the recording chamber. The descending aorta was cannulated with a double-lumen catheter for perfusion and measurement of perfusion pressure. The preparation was perfused with aCSF containing sucrose (4.5×10^{-3} g/mL) for oncotic pressure, warmed to 31 °C using a peristaltic pump, recirculating water bath and heat exchanger (ELMI, TW-2.02). The perfusion circuit also contained two bubble traps and a nylon filter (Millipore, 100 µm pore size) to prevent embolia. The perfusate was continually bubbled with carbogen (95% O_2/5% CO_2) to maintain constant chemosensory drive. Phrenic and hypoglossal nerves were mounted in suction electrodes to measure the inspiratory motor pattern. Nerve potentials were amplified (10,000×, Warner Instruments, DP-311), filtered (0.01–10 kHz), digitized (AD Instruments, PowerLab 16/35, 2 kHz sampling frequency) and stored on a computer using LabChart software (AD Instruments).

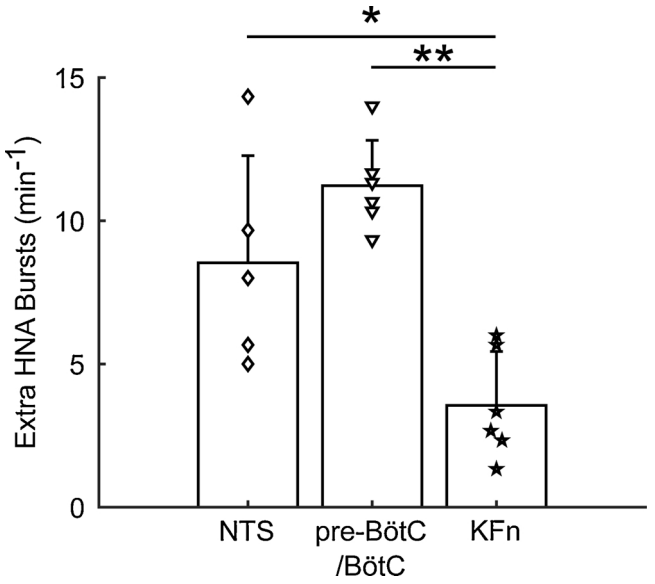

Fig. 2. Extra HNA bursts occurred more frequently after local disinhibition of the NTS or pre-BötC/BötC **than after local disinhibition of the KFn.** To further examine the effect of local disinhibition of the NTS, pre-BötC/BötC or KFn on extra HNA bursts that occurred out-of-phase with PNA, we manually scored the rate of occurrence of these events after local disinhibition of each target site. Extra HNA bursts occurred more frequently after local disinhibition of the NTS or pre-BötC/BötC compared to after local disinhibition of the KFn. * $p < 0.05$; ** $p < 0.01$.

2.2. Experimental protocol

After the initial stabilization of the eupneic three-phase respiratory rhythm, we recorded 10 min of the baseline inspiratory motor pattern. In the present work, we investigated the role of the NTS (N = 5 preparations), pre-BötC/BötC (N = 6 preparations), KFn (N = 6 preparations) in controlling the spinal and cranial inspiratory motor pattern. To functionally identify the target site coordinates, using a triple barreled pipette, we first mapped the target site with glutamate microinjections (50 nL, 10 mM). Next, we microinjected bicuculline (50 nL, 10 mM), a GABA(A) receptor antagonist, to locally disinhibit and consequently locally increase the excitability of the target site. Next, we microinjected pontamine sky blue (50 nL, 2% w/v in aCSF) for *post-hoc* histologic verification of injection site locations. This procedure was repeated on the contralateral side. We recorded 10 min of the inspiratory motor pattern after local disinhibition of the target site to characterize the effect of the perturbation on inspiratory motor pattern formation.

At the end of the experiment, brainstems were removed, post-fixed in paraformaldehyde (4% w/v in PBS), cryoprotected in sucrose (20% w/v in PBS), cryosectioned (50 µm thickness) and counterstained with neutral red to verify the anatomic location of the microinjection sites (Fig. 5).

2.3. Data analysis

A prominent effect evoked by modulating local excitability within the brainstem respiratory network was the occurrence of extra HNA bursts that had an anti-phasic relationship with PNA. Thus, we first manually scored the rate of occurrence of this respiratory motor pattern motif during three-minute epochs acquired after local disinhibiton of the NTS, pre-BötC/BötC or KFn.

2.3.1. Cycle-triggered averages

We qualitatively analyzed the phrenic and hypoglossal motor pattern before and after local disinhibition by comparing cycle triggered averages. To generate cycle-tirggered averages of PNA and HNA, the signals were first high-pass filtered to remove DC fluctuations with a zero-phase FIR filter (300 Hz), rectified and integrated (100 ms time-constant). We next used a threshold crossing algorithm to detect the offset times of PNA (inspiratory off-switch; inspiration to post-inspiration transition). Events were manually inspected to ensure that no false positive cycles were included in subsequent analyses. Using these event times, we computed the mean and standard deviation of PNA and HNA within a 9 s window surrounding the inspiratory off-switch.

2.3.2. Phase synchronization analysis

To quantify the strength of the phase synchronization interaction between PNA and HNA and to determine the significance of the interaction, we band-pass filtered the integrated signals around the respiratory frequency (0.1–0.5 Hz). Next, instantaneous protophases were extracted by applying the Hilbert transform. Instantaneous phases were then determined by applying the transformation defined in (Kralemann et al., 2008). To quantify the strength of phase synchronization between PNA and HNA, we computed the mutual information of their instantaneous phases (Dhingra et al., 2017; Zhu et al., 2013). Mutual information, a measure of the statistical dependence between two variables, was computed from the joint-probability histogram according to the following equation:

$$I(\varphi_{PNA}; \varphi_{HNA}) = -\int_0^{2\pi}\int_0^{2\pi} P(\varphi_{PNA}, \varphi_{HNA}) \ln \frac{P(\varphi_{PNA}, \varphi_{HNA})}{P(\varphi_{PNA})P(\varphi_{HNA})} d\varphi_{PNA} d\varphi_{HNA}$$

where $P(\varphi_{PNA}, \varphi_{HNA})$ is the joint probability distribution of the instantaneous phases, and $P(\varphi_{PNA})$ and $P(\varphi_{HNA})$ are the marginal probability distributions of either variable. For all measurements of the mutual information of the instantaneous phases, we used a fixed bin width of 0.03 rad to discretize the probability distributions. Because we use the natural logarithm in computing mutual information, reported mutual information values are presented in the corresponding unit of nats. Values of mutual information near zero indicate that the variables are independent and have no coupling, whereas high values of mutual information are associated with high dependence between the instantaneous phase variables, and thereby associated with a high synchronization strength between the pair of motor outputs.

To assess whether the observed synchronization measurement was statistically significant, we compared the original mutual information measurement with that of a bootstrap distribution that represented the null hypothesis that the two instantaneous phases were independent. For each observed mutual information measurement, a bootstrap distribution was generated by randomly shuffling the inter-event intervals and re-computing the instantaneous phases—thereby preserving the periodicity of the original signals—and their mutual information. The bootstrapping procedure was repeated 100 times to estimate the distribution that represented the null hypothesis. If an epoch had an original mutual information greater than the 99% confidence interval of the mutual information values in its associated bootstrap distribution, it was considered significant.

All analyses were performed using custom routines implemented in MATLAB. All measurements are reported as the mean ± standard deviation. Unless stated otherwise, statistical comparisons were made by applying a repeated measures ANOVA, and the Tukey HSD post-hoc test to identify specific differences.

3. Results

To investigate the influence of excitation-inhibition balance within the NTS, pre-BötC/BötC or KFn on phrenic and hypoglossal motor patterns, we recorded these motor patterns before and after local disinhibition of each target site. Representative traces are shown before and after local disinhibition in Fig. 1. At baseline (Fig. 1A, C & E), we observed the typical interaction between PNA and HNA such that HNA

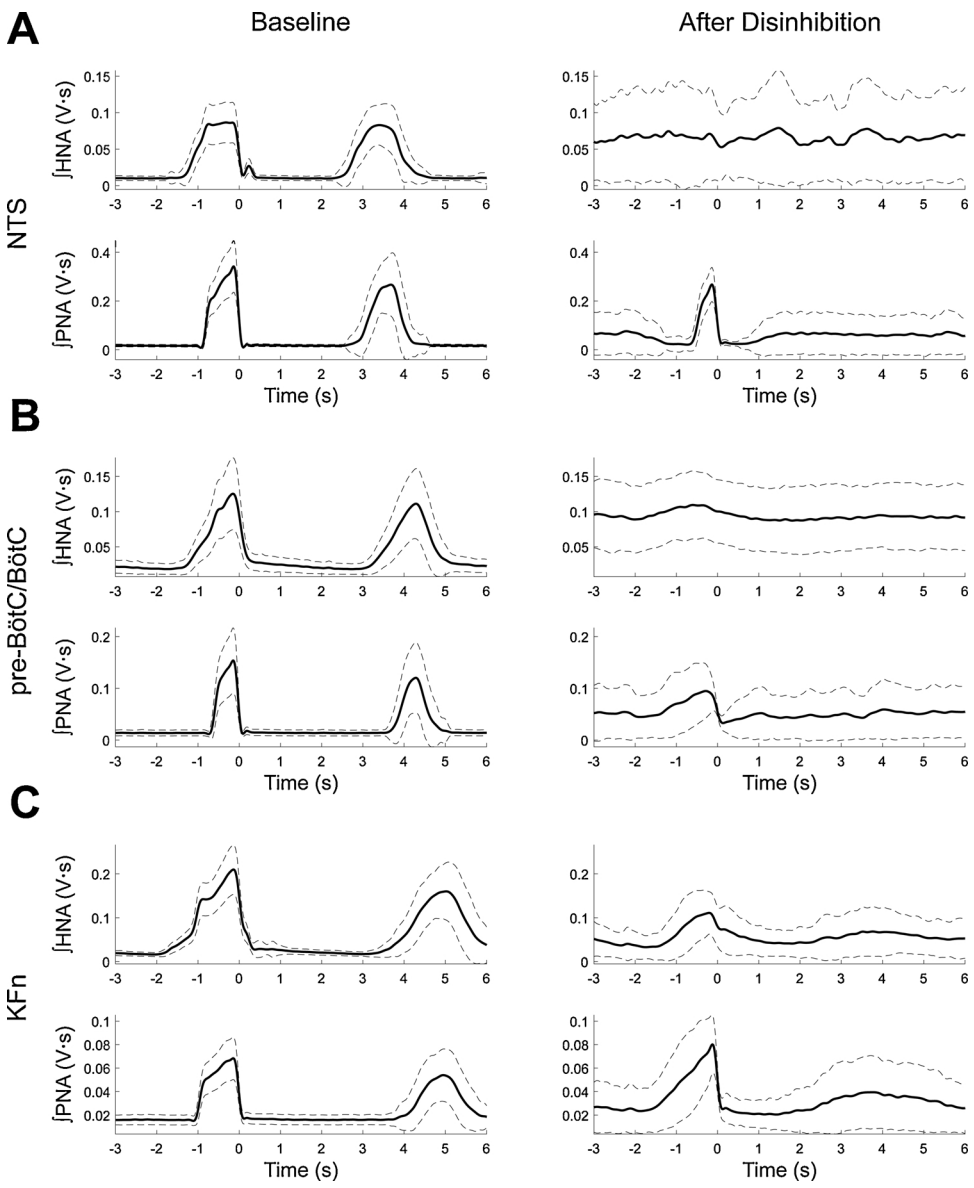

Fig. 3. Spinal PNA & cranial HNA became more uncoupled after local disinhibition of the NTS or pre-BötC/BötC **than after local disinhibition of the KFn.** To compare the average pattern of spinal PNA and cranial HNA before and after local disinhibition of each target site, we computed cycle-triggered averages of these two inspiratory motor outputs triggered via the inspiratory off-switch (inspiration-to-post-inspiration/I-Off transition). Thick black lines indicate the average nerve activity during the 9 s window, whereas dashed black lines indicate the standard deviation of the mean. At baseline (A, B & C, left panels), all preparations showed the typical eupneic pattern of inspiratory activities such that HNA began discharging during pre-inspiration, whereas PNA discharge was confined to the inspiratory phase. After local disinhibition of the NTS (A, right panel), I-Off triggered HNA was constant throughout the averaging window. Note that this does not imply that there was tonic HNA discharge after local disinhibition of the NTS. Instead, the observation suggests that the relationship between PNA and HNA became less predictable (or more variable) such that an I-Off trigger calculated from PNA did not have a constant relationship with HNA bursts at any point within the averaging window. After local disinhibition of the pre-BötC/BötC (B, right panel), I-Off triggered HNA was also almost constant throughout the averaging window. However, a small burst of HNA still appeared simultaneously with PNA, suggesting that the degree of uncoupling between spinal and cranial inspiratory motor outflows was slightly less than that evoked by local disinhibition of the NTS. Finally, after local disinhibition of the KFn (C, right panel), cycle triggered averages continued to show simultaneous bursts of HNA and PNA during inspiration suggesting that the degree of uncoupling between PNA and HNA was less than that evoked by local disinhibition of either the NTS or pre-BötC/BötC.

begins before PNA during pre-inspiration (pre-I), and both show activity throughout the inspiratory phase (for example, see shaded bars in Fig. 1A) of the respiratory cycle. We rarely observed HNA during the post-inspiratory phase, though this can occur occasionally. After local disinhibition of the NTS (Fig. 1B), inspiratory bursts of PNA became shorter and more variable. In contrast, after local disinhibition of the NTS, HNA was enhanced and often occurred out of phase with PNA, though HNA bursts were also observed synchronously with inspiratory PNA (compare HNA during and between shaded gray bars in Fig. 1B). After local disinhibition of the pre-BötC/BötC core of the respiratory network (Fig. 1D), the burst shape of PNA became more variable. In addition, the PNA inter-burst intervals were also reduced and more variable. Local disinhibition of the pre-BötC/BötC evoked bursts of HNA that occurred both phasically and anti-phasically with PNA, and enhanced tonic HNA. Local disinhibition of the KFn (Fig. 1F) increased the variability of PNA burst duration with some PNA bursts being prolonged and others being truncated. However, local disinhibition of the KFn had a weaker effect on HNA. While some anti-phasic HNA was observed, the majority of HNA was synchronous with PNA. Finally, after local disinhibition of any target site, we rarely observed pre-inspiratory HNA that preceded PNA discharge.

To further analyze the effect of local disinhibition of the NTS, pre-BötC/BötC or KFn on the presence of HNA bursts that occurred phasically or anti-phasically with PNA bursts, we manually scored the occurrence of extra bursts of HNA that were anti-phasic with respect to PNA (Fig. 2). For the group, extra HNA bursts that were out of phase with PNA occurred significantly more frequently after local disinhibition of the NTS compared to after local disinhibition of the KFn (after local disinhibition of the NTS, 8.5 ± 3.7 bursts/min *versus* after local disinhibition of the KFn, 3.6 ± 1.9 bursts/min, $p < 0.05$). Similarly, extra HNA bursts also occurred more frequently after local disinhibition of the pre-BötC/BötC compared to after local disinhibition of the KFn (after local disinhibition of the pre-BötC/BötC, 11.2 ± 1.6 bursts/min *versus* after local disinhibition of the KFn, 3.6 ± 1.9 bursts/min, $p < 0.01$).

To qualitatively compare the average pattern of PNA and HNA before and after local disinhibition of the NTS, pre-BötC/BötC or KFn, we computed inspiratory-off switch-triggered averages of PNA and HNA (Fig. 3). At baseline (Fig. 3, *left panels*), all preparations showed the expected pattern of a sharply rising, and subsequently ramp-like discharge of PNA that defines the inspiratory phase of the respiratory motor pattern. Similarly, all preparations showed the expected pattern of HNA wherein HNA begins during pre-I and continues until the end of inspiration.

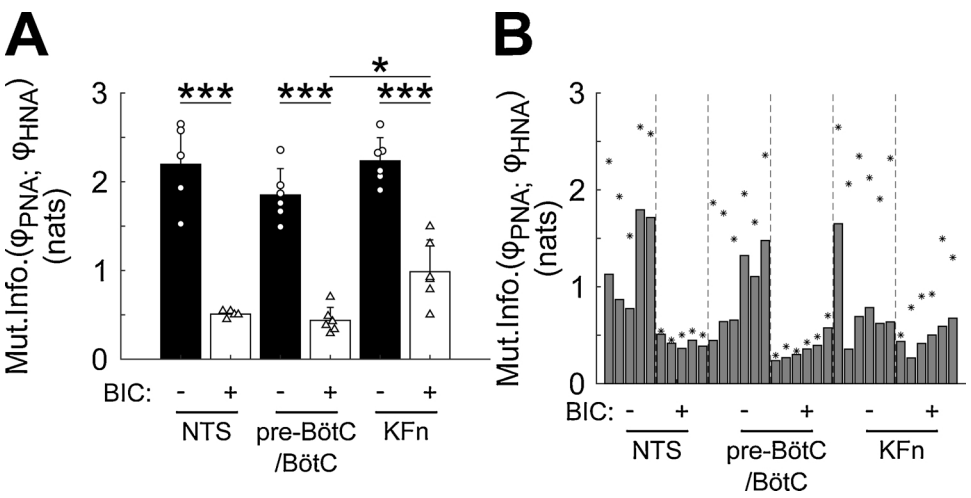

Fig. 4. Local disinhibition of the NTS or pre-BötC/BötC evoked a stronger uncoupling of spinal PNA and cranial HNA inspiratory motor outputs than local disinhibition of the KFn. To quantitatively analyze the effects of local disinhibition of the NTS, pre-BötC/BötC or KFn on the coupling between spinal PNA and cranial HNA inspiratory motor outputs, we measured the strength of phase synchronization (mutual information of the instantaneous phases; A & B) between PNA and HNA before and after local disinhibition of each target site. For the group, local disinhibition of any target site significantly reduced the strength of phase synchrony between PNA and HNA (A). Consistent with previous observations analyzing the occurrence of extra HNA bursts and the PNA I-Off triggered averages of HNA after local disinhibition, local disinhibition of the pre-BötC/BötC evoked a significantly stronger uncoupling of PNA and HNA compared to local disinhibition of the KFn. Similarly, local disinhibition of the NTS also tended to evoke a stronger uncoupling of PNA and HNA compared to local disinhibition of the KFn. To assess whether the observed phase synchronization interactions were significant, we compared the observed mutual information values with those computed from a surrogate distribution in which the underlying data was shuffled but maintained the same periodicity as the original data (B). In all cases, even after local disinhibition of any target site, the measured mutual information of the instantaneous phases (asterisks) was greater than the 99% confidence interval of the surrogate distribution (gray bars) suggesting the presence of a significant phase synchronization interaction between spinal and cranial inspiratory motor outputs. * $p < 0.05$; *** $p < 0.001$.

After local disinhibition of any target site, the variability of PNA and HNA increased. This was reflected by both the flatness of the averaged HNA pattern and the standard deviation of the averaged HNA pattern (compare the dashed lines, *e.g.*, the standard deviation of HNA or PNA, in Fig. 3A–C, *right panels*). After local disinhibition of the NTS (Fig. 3A, *right*), PNA bursts (*bottom right panel*) became shorter. Moreover, the onset of the subsequent PNA burst became highly variable such that the standard deviation of PNA abruptly increased within 1 s after the end of the triggered-burst. In contrast, average HNA activity no longer maintained any burst-like discharge, and instead appeared tonic throughout the window (Fig. 3A, *top right panel*). Note that this does not imply that there was tonic HNA discharge after local disinhibition of the NTS. Instead, the observation suggests that the relationship between PNA and HNA became less predictable (or more variable) such that an inspiratory off-switch event in PNA did not have a constant relationship with HNA bursts at any point within the averaging window. After local disinhibition of the pre-BötC/BötC (Fig. 3B, *right*), the amplitude and variability of PNA was further reduced compared to disinhibition of the NTS. With respect to HNA, local disinhibition of the pre-BötC/BötC evoked a pattern of HNA that appeared tonic across a respiratory cycle but maintained a burst that was synchronous with inspiratory PNA. Finally, after local disinhibition of the KFn, PNA became more variable and appeared ramp-like due to the variability in the inspiratory off-switch (see representative traces in Fig. 1F). However, the peak amplitude of PNA remained similar to that observed at baseline. Local disinhibition of the KFn had a lesser effect on HNA compared to local disinhibition of the NTS or pre-BötC/BötC. Though the cycle triggered average of HNA was more variable after local disinhibition of the KFn, the average HNA pattern had a larger inspiratory burst and stronger offset compared to the HNA patterns evoked by local disinhibition of the NTS or pre-BötC/BötC.

Finally, to quantify the effect of local disinhibition of the NTS, pre-BötC/BötC or KFn on the coupling between PNA and HNA, we measured the strength of synchronization and the relative phase difference between PNA and HNA (Fig. 4). Mutual information quantifies the dependence between two variables. As such, synchronization between two instantaneous phase variables leads to higher levels of mutual information, whereas the absence of synchronization between two instantaneous phase variables yields lower values of mutual information. At baseline, we observed high values of mutual information that suggested the presence of a strong phase synchronization interaction between PNA and HNA. After local disinhibition of any target site, the strength of the phase synchronization between PNA and HNA was significantly reduced (NTS: at baseline, 2.19 ± 0.47 nats *versus* after local disinhibition, 0.51 ± 0.04 nats $p < 0.001$; pre-BötC/BötC: at baseline, 1.85 ± 0.30 nats *versus* after local disinhibition, 0.44 ± 0.15 nats $p < 0.001$; KFn: at baseline, 2.24 ± 0.26 nats *versus* after local disinhibition, 0.99 ± 0.36 nats $p < 0.001$; Fig. 4A). Further, local disinhibition of the pre-BötC/BötC evoked a stronger reduction in the strength of synchronization between PNA and HNA compared to that evoked by local disinhibition of the KFn (after local disinhibition of the pre-BötC/BötC, 0.44 ± 0.15 nats *versus* after local disinhibition of the KFn, 0.99 ± 0.36 nats, $p < 0.05$). Similarly, there was a tendency for local disinhibition of the NTS to evoke a stronger reduction in the strength of synchronization between PNA and HNA compared to that evoked by local disinhibition of the KFn, though this difference was not significant.

Next, to confirm that the measured synchronization interactions were indeed significant, we compared the observed mutual information between the instantaneous phases of PNA and HNA with that of surrogate distributions for the statistic in which the underlying data was shuffled before computing the mutual information (Fig. 4B). In all cases, even after local disinhibition, the measured mutual information between HNA and PNA was greater than the 99% confidence interval of the surrogate distribution suggesting the presence of a significant phase synchronization interaction between PNA and HNA, even after the strong perturbation of the eupneic respiratory motor pattern. This observation suggests that the distributed organization of the brainstem respiratory network is sufficient to partially compensate for local perturbations of excitation-inhibition balance.

4. Discussion

In the present study, we have shown that increasing local circuit excitability via disinhibition of either the NTS, pre-BötC/BötC or KFn was sufficient to perturb and desynchronize the spinal and cranial inspiratory motor pattern. Qualitatively, the nature of the disruption evoked by local disinhibition differed between medullary and pontine target sites such that stronger disruptions in HNA patterning were evoked by local disinhibition of medullary target sites. Quantitatively, local disinhibition of any target site was sufficient to reduce the strength of phase synchronization between PNA (spinal) and HNA

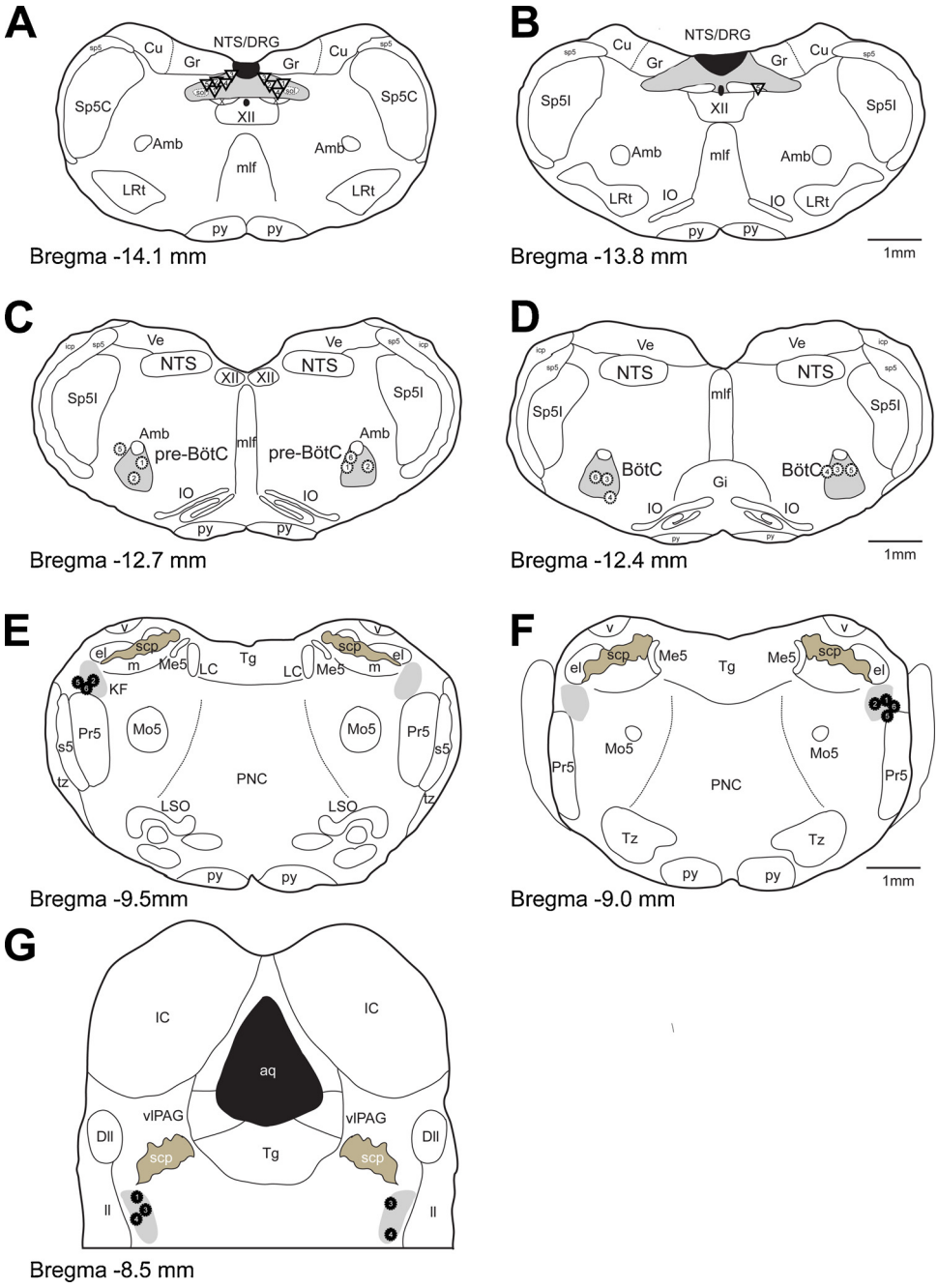

Fig. 5. Histologic verification of the injection sites. The localization of the bicuculline injection sites was confirmed histologically by identifying the location of the pontamine sky blue injections. Schematic drawings depicting those locations are shown above (A–G). Triangles denote the location of NTS injection sites. White-filled circles denote the locations of pre-BötC/BötC injection sites. Black-filled circles denote the locations of the KFn injection sites.

(cranial) inspiratory motor outputs. However, local disinhibition of medullary target sites had a greater effect on the phase synchrony between PNA and HNA compared to local disinhibition of the KFn.

Here, we discuss the technical limitations of the present study. First, we used local disinhibition (blockade of GABA(A)Rs) to locally increase neuronal excitability within anatomically-distinct nuclei of the ponto-medullary respiratory network of the *in situ* perfused preparation. While our results suggest that locally increasing neuronal excitability in the NTS, pre-BötC/BötC or KFn was sufficient to perturb the respiratory motor pattern *in situ*, the methods preclude the identification of the sources of GABAergic inputs to these areas, *i.e.*, GABAergic inhibition of these areas could arise either locally from within the target nucleus or arise from other brainstem respiratory nuclei. Second, because the *in situ* preparation lacks critical chemo- and mechano-sensory feedback, it enables the investigation of the central-, but not peripheral-, mechanisms of respiratory pattern formation. While sensory feedback, especially vagal mechano-sensory (Hering-Breuer) feedback from the lungs, is well known to modulate the respiratory motor pattern, a previous study disinhibited the pre-BötC and BötC *in vivo* and observed that this perturbation suppressed the vagal Hering-Breuer reflex suggesting that the results of the present study may also generalize to the *in vivo* setting (Janczewski et al., 2013). Interestingly, despite blocking both GABAergic and glycinergic transmission in these areas, the authors did not observe a similar modulation of the respiratory pattern. Together, these observations suggest that other sensory feedback inputs or descending inputs from higher brain regions may act to stabilize the respiratory pattern after local modulation of neuronal excitability *in vivo*. Finally, in the present study, we reasoned that the strength of synchronization

between respiratory motor outputs could be used to quantify the magnitude of local disinhibition-evoked changes in the respiratory pattern. Consistent with this assumption, we observed near perfect synchronization between PNA and HNA at baseline, and a reduction of the strength of synchrony after local disinhibition of any brainstem target area. While synchronization of respiratory motor outputs could arise via synaptic coupling between independent phase-specific oscillators, this is not a consensus view in the field. Another, perhaps more likely, possibility is that synchronization between respiratory motor outputs arises because respiratory motor pools may share common inputs from brainstem areas that comprise the distributed respiratory network.

In the present study, we frequently observed extra HNA bursts that occurred during expiratory intervals after local disinhibition of the NTS or pre-BötC/BötC compared to their penetrance after local disinhibition of the KFn. However, we note that disruption of the balance of excitatory and inhibitory synaptic activity (EI balance) within the KFn area also significantly transformed inspiratory PNA-HNA patterning. During control conditions, HNA displays pronounced pre-inspiratory activity that drives the protrusion of the tongue which in turn reduces upper airway resistance prior to the active inspiratory phase. Pre-inspiratory HNA could no longer be detected after bicuculline microinjections into the KFn. We suggest that the effect of a disturbed EI-balance in the KFn may have disinhibited the normally suppressed pre-inspiratory drive to PNA resulting in simultaneous inspiratory HNA and PNA bursts. Nevertheless, the simultaneous PNA and HNA became more variable in duration after perturbation of EI balance in the KFn. The variable PNA duration is generally in line with the role of the KFn in the mediation of the inspiratory off-switch (I-Off switch, see Cohen and Shaw, 2004; Dutschmann and Dick, 2012; Dutschmann and Herbert, 2006; Mörschel and Dutschmann, 2009; Smith et al., 2013, 2007; von Euler, 1983). Thus, the present data suggest that disturbed EI balance consequently affects the timing of I-Off switch. The role of the KFn in specifically gating HNA premotor and motor activity was also reported previously (Bautista and Dutschmann, 2014; Dutschmann et al., 2007).

The greater susceptibility of observing extra HNA bursts after medullary perturbations of EI balance compared to the pons might be related to the anatomic proximity or structural overlap of both the NTS and pre-BötC/BötC with other functionally different motor CPGs (see Bianchi and Gestreau, 2009; Ramirez and Baertsch, 2018). Thus, local disinhibition of these medullary brainstem areas may have triggered extra HNA bursts in the context of orofacial behavior (Bartlett and Leiter, 2012; Gestreau et al., 2005). In a recent experimental and computational study of hypoxia-evoked modulation of the respiratory pattern, the author's observed that post-inspiratory HNA was evoked during exposure to acute hypoxia (Barnett et al., 2017). In their simulations, the authors showed that the hypoxia-evoked post-inspiratory discharge in HNA depended on excitatory inputs from the NTS and inhibitory inputs from the BötC to pre-motor post-inspiratory neurons. Their results suggest that disinhibition of chemosensory neurons in the NTS may also account for the emergence of extra HNA bursts in the present study. Therefore, we speculate that some component of the extra HNA bursts were indeed related to the disinhibition of non-respiratory orofacial CPGs or sensory reflex pathways.

In addition to ponto-medullary differences in the patterning of HNA, we also observed a differential regulation of the strength of synchronization between HNA and PNA. Disinhibition of the pre-BötC/BötC area or NTS evoked a greater decrease in the strength of phase synchrony compared to disinhibition of the KFn. Thus, circuit mechanisms underlying the patterning of inspiratory spinal and cranial motor outputs seem to be predominantly localized to the medulla. This observation contrasts with the findings of our most recent study (Dhingra et al., 2019) in which we observed that disinhibition of either the NTS, pre-BötC/BötC or KFn evoked a comparable decrease in the strength of phase synchrony between inspiratory PNA and post-inspiratory vagal nerve activity. Note that post-inspiratory motor activity driving laryngeal adductors occurs during the early phase of expiration when it counteracts the maximal recoil force of the expanded lungs to smooth expiratory airflow (see Dutschmann et al., 2014). The observation that the pattern generating network underlying inspiratory *versus* that underlying inspiratory and post-inspiratory motor patterns is consistent with a recent comparative study in bullfrogs that also suggested that interaction between three oscillator networks was necessary to generate the respiratory motor pattern (Baghdadwala et al., 2015). Thus, the findings of the present study support the working hypothesis that inspiratory pattern formation mechanisms may be more localized to the medulla, whereas expiratory pattern formation mechanisms seem to be more distributed across the pons and medulla.

Acknowledgement

This work was supported by a Discovery project funded by the Australian Research Council [DP170104861].

References

Baghdadwala, M.I., Duchcherer, M., Paramonov, J., Wilson, R.J.A., 2015. Three brainstem areas involved in respiratory rhythm generation in bullfrogs. J. Physiol. 593, 2941–2954. https://doi.org/10.1113/JP270380.

Barnett, W.H., Abdala, A.P., Paton, J.F.R., Rybak, I.A., Zoccal, D.B., Molkov, Y.I., 2017. Chemoreception and neuroplasticity in respiratory circuits. Exp. Neurol. 287, 153–164. https://doi.org/10.1016/j.expneurol.2016.05.036. Special Issue: Respiratory Neuroplasticity.

Bartlett, D., 1989. Respiratory functions of the larynx. Physiol. Rev. 69, 33–57. https://doi.org/10.1152/physrev.1989.69.1.33.

Bartlett, D., Leiter, J.C., 2012. Coordination of breathing with nonrespiratory activities. Comprehensive Physiology. American Cancer Society, pp. 1387–1415. https://doi.org/10.1002/cphy.c110004.

Bautista, T.G., Dutschmann, M., 2014. Inhibition of the pontine Kölliker-Fuse nucleus abolishes eupneic inspiratory hypoglossal motor discharge in rat. Neuroscience 267, 22–29. https://doi.org/10.1016/j.neuroscience.2014.02.027.

Bianchi, A.L., Gestreau, C., 2009. The brainstem respiratory network: an overview of a half century of research. Respir. Physiol. Neurobiol. 168, 4–12. https://doi.org/10.1016/j.resp.2009.04.019.

Cohen, M.I., Shaw, C.-F., 2004. Role in the inspiratory off-switch of vagal inputs to rostral pontine inspiratory-modulated neurons. Respir. Physiol. Neurobiol. 143, 127–140. https://doi.org/10.1016/j.resp.2004.07.017.

Del Negro, C.A., Funk, G.D., Feldman, J.L., 2018. Breathing matters. Nat. Rev. Neurosci. 1. https://doi.org/10.1038/s41583-018-0003-6.

Dhingra, R.R., Dutschmann, M., Galán, R.F., Dick, T.E., 2017. Kölliker-Fuse nuclei regulate respiratory rhythm variability via a gain-control mechanism. Am. J. Physiol. – Regul. Integr. Comp. Physiol. 312, R172–R188. https://doi.org/10.1152/ajpregu.00238.2016.

Dhingra, R.R., Furuya, W.I., Bautista, T.G., Dick, T.E., Galan, R.F., Dutschmann, M., 2019. Increasing local excitability of brainstem respiratory nuclei reveals a distributed network underlying respiratory motor pattern formation. Front. Auton. Neurosci in revision.

Dutschmann, M., Dick, T.E., 2012. Pontine mechanisms of respiratory control. Compr. Physiol. 2, 2443–2469. https://doi.org/10.1002/cphy.c100015.

Dutschmann, M., Herbert, H., 2006. The Kölliker-Fuse nucleus gates the postinspiratory phase of the respiratory cycle to control inspiratory off-switch and upper airway resistance in rat. Eur. J. Neurosci. 24, 1071–1084. https://doi.org/10.1111/j.1460-9568.2006.04981.x.

Dutschmann, M., Paton, J.F.R., 2002. Glycinergic inhibition is essential for co-ordinating cranial and spinal respiratory motor outputs in the neonatal rat. J. Physiol. 543, 643–653. https://doi.org/10.1113/jphysiol.2001.013466.

Dutschmann, M., Wilson, R.J.A., Paton, J.F.R., 2000. Respiratory activity in neonatal rats. Auton. Neurosci. 84, 19–29. https://doi.org/10.1016/S1566-0702(00)00177-6.

Dutschmann, M., Kron, M., Mörschel, M., Gestreau, C., 2007. Activation of Orexin B receptors in the pontine Kölliker-Fuse nucleus modulates pre-inspiratory hypoglossal motor activity in rat. Respir. Physiol. Neurobiol. 159, 232–235. https://doi.org/10.1016/j.resp.2007.06.004.

Dutschmann, M., Jones, S.E., Subramanian, H.H., Stanic, D., Bautista, T.G., 2014. The physiological significance of postinspiration in respiratory control. Prog. Brain Res. Breath. Emot. Evol. 212, 113–130. https://doi.org/10.1016/B978-0-444-63488-7.00007-0.

Gestreau, C., Dutschmann, M., Obled, S., Bianchi, A.L., 2005. Activation of XII motoneurons and premotor neurons during various oropharyngeal behaviors. Respir. Physiol. Neurobiol. 147, 159–176. https://doi.org/10.1016/j.resp.2005.03.015.

Iscoe, S., 1998. Control of abdominal muscles. Prog. Neurobiol. 56, 433–506. https://doi.org/10.1016/S0301-0082(98)00046-X.

Janczewski, W.A., Tashima, A., Hsu, P., Cui, Y., Feldman, J.L., 2013. Role of inhibition in respiratory pattern generation. J. Neurosci. 33, 5454–5465. https://doi.org/10.1523/JNEUROSCI.1595-12.2013.

Kralemann, B., Cimponeriu, L., Rosenblum, M., Pikovsky, A., Mrowka, R., 2008. Phase dynamics of coupled oscillators reconstructed from data. Phys. Rev. E 77. https://doi.org/10.1103/PhysRevE.77.066205.

Molkov, Y.I., Abdala, A.P.L., Bacak, B.J., Smith, J.C., Paton, J.F.R., Rybak, I.A., 2010. Late-expiratory activity: emergence and interactions with the respiratory CPG. J. Neurophysiol. 104, 2713–2729. https://doi.org/10.1152/jn.00334.2010.

Mörschel, M., Dutschmann, M., 2009. Pontine respiratory activity involved in inspiratory/expiratory phase transition. Philos. Trans. R. Soc. B Biol. Sci. 364, 2517–2526. https://doi.org/10.1098/rstb.2009.0074.

Paton, J.F.R., 1996. A working heart-brainstem preparation of the mouse. J. Neurosci. Methods 65, 63–68. https://doi.org/10.1016/0165-0270(95)00147-6.

Pisanski, A., Pagliardini, S., 2018. The parafacial respiratory group and the control of active expiration. Respir. Physiol. Neurobiol. https://doi.org/10.1016/j.resp.2018.06.010.

Ramirez, J.-M., Baertsch, N.A., 2018. The dynamic basis of respiratory rhythm generation: one breath at a time. Annu. Rev. Neurosci. https://doi.org/10.1146/annurev-neuro-080317-061756.

Richter, D.W., Smith, J.C., 2014. Respiratory rhythm generation in vivo. Physiology 29, 58–71. https://doi.org/10.1152/physiol.00035.2013.

Sant'Ambrogio, G., Tsubone, H., Sant'Ambrogio, F.B., 1995. Sensory information from the upper airway: role in the control of breathing. Respir. Physiol. 102, 1–16. https://doi.org/10.1016/0034-5687(95)00048-I.

Smith, J.C., Abdala, A.P.L., Koizumi, H., Rybak, I.A., Paton, J.F.R., 2007. Spatial and functional architecture of the mammalian brain stem respiratory network: a hierarchy of three oscillatory mechanisms. J. Neurophysiol. 98, 3370–3387. https://doi.org/10.1152/jn.00985.2007.

Smith, J.C., Abdala, A.P.L., Rybak, I.A., Paton, J.F.R., 2009. Structural and functional architecture of respiratory networks in the mammalian brainstem. Philos. Trans. Biol. Sci. 364, 2577–2587.

Smith, J.C., Abdala, A.P.L., Borgmann, A., Rybak, I.A., Paton, J.F.R., 2013. Brainstem respiratory networks: building blocks and microcircuits. Trends Neurosci. 36, 152–162. https://doi.org/10.1016/j.tins.2012.11.004.

von Euler, C., 1983. On the central pattern generator for the basic breathing rhythmicity. J. Appl. Physiol. 55, 1647–1659. https://doi.org/10.1152/jappl.1983.55.6.1647.

Widdicombe, J.G., 1982. Pulmonary and respiratory tract receptors. J. Exp. Biol. 100, 41–57.

Zhu, Y., Hsieh, Y.-H., Dhingra, R.R., Dick, T.E., Jacono, F.J., Galán, R.F., 2013. Quantifying interactions between real oscillators with information theory and phase models: application to cardiorespiratory coupling. Phys. Rev. E 87. https://doi.org/10.1103/PhysRevE.87.022709.